Cell, Vol. 117, 387–398, April 30, 2004, Copyright ©2004 by Cell Press

ATF4 Is a Substrate of RSK2 and an Essential Regulator of Osteoblast Biology: Implication for Coffin-Lowry Syndrome

Xiangli Yang,[1] Koichi Matsuda,[1] Peter Bialek,[1] Sylvie Jacquot,[2] Howard C. Masuoka,[3] Thorsten Schinke,[1] Lingzhen Li,[1] Stefano Brancorsini,[2] Paolo Sassone-Corsi,[2] Tim M. Townes,[3] Andre Hanauer,[2] and Gerard Karsenty[1,*]

[1]Department of Molecular and Human Genetics and Bone Disease Program of Texas
Baylor College of Medicine
Houston, Texas 77030

[2]Institut de Genetique et de Biologie Moleculaire et Cellulaire
C.U. de Strasbourg
67404 Illkirch Cedex
France

[3]Department of Biochemistry and Molecular Genetics
University of Alabama at Birmingham
Birmingham, Alabama 35294

Summary

Coffin-Lowry Syndrome (CLS) is an X-linked mental retardation condition associated with skeletal abnormalities. The gene mutated in CLS, *RSK2*, encodes a growth factor-regulated kinase. However, the cellular and molecular bases of the skeletal abnormalities associated with CLS remain unknown. Here, we show that RSK2 is required for osteoblast differentiation and function. We identify the transcription factor ATF4 as a critical substrate of RSK2 that is required for the timely onset of osteoblast differentiation, for terminal differentiation of osteoblasts, and for osteoblast-specific gene expression. Additionally, RSK2 and ATF4 posttranscriptionally regulate the synthesis of Type I collagen, the main constituent of the bone matrix. Accordingly, *Atf4*-deficiency results in delayed bone formation during embryonic development and low bone mass throughout postnatal life. These findings identify ATF4 as a critical regulator of osteoblast differentiation and function, and indicate that lack of ATF4 phosphorylation by RSK2 may contribute to the skeletal phenotype of CLS.

Introduction

An efficient means to identify transcription factors determining skeletal cell differentiation has been the molecular elucidation of human skeletal dysplasias with a dominant mode of inheritance. This contributed, for instance, to the identification of *Sox9* and *Runx2* as initiators of chondrocyte and osteoblast differentiation, respectively (Kwok et al., 1995; Lee et al., 1997; Mundlos et al., 1997). Other skeletal dysplasias that are inherited either in a recessive manner or in a dominant manner with reduced penetrance have a milder phenotype than campomelic or cleidocranial dysplasia, the diseases caused by *Sox9* or *Runx2* haploinsufficiency. Such milder phenotypes imply that the genes mutated in these diseases may act later during skeletogenesis than *Sox9* or *Runx2*. One skeletal dysplasia inherited in a dominant fashion with reduced penetrance is Coffin-Lowry Syndrome (CLS), an X-linked mental retardation condition with delayed bone age, delayed closure of fontanelles, and short stature (Coffin et al., 1966; Lowry et al., 1971).

The gene mutated in CLS, *RSK2,* encodes a growth factor-regulated kinase. RSK2 belongs to a family of ribosomal serine/threonine kinases that contain two distinct kinase domains, one at the C-terminal and one at the N-terminal (Trivier et al., 1996; Xing et al., 1996; Frodin et al., 2000). ERK phosphorylation of RSK2 C-terminal domain results in the activation of the N-terminal kinase domain, which can then phosphorylate its substrates (Fisher and Blenis, 1996; Dalby et al., 1998). In vitro, RSK2 phosphorylates CREB and is required for growth-factor-stimulated transcription of *c-Fos* (Xing et al., 1996; Bruning et al., 2000). CREB phosphorylation, however, is not altered and *c-Fos* expression increases normally following exercise in *Rsk2*-deficient mice (Dufresne et al., 2001) suggesting that RSK2 has other substrates.

Besides molecular elucidation of human skeletal dysplasias other experimental approaches have been used with great success to improve our understanding of cell differentiation during skeletogenesis. One of them is the analysis of regulatory sequences in cell-specific genes followed by verification of findings generated by these studies through mouse genetics. This also led for instance to the identification of Runx2 as an osteoblast differentiation factor (Ducy et al., 1997).

Using a combination of human genetic information, analysis of mutant mouse strains, and molecular studies, we show here that RSK2 is required for osteoblast differentiation and function in vivo and provide molecular and genetic evidence that ATF4 is a substrate of RSK2 in osteoblasts. We also show that ATF4 regulates several aspects of osteoblast biology ranging from onset of differentiation to cell-specific gene expression. Moreover, ATF4 and RSK2 regulate Type I collagen synthesis through a posttranscriptional mechanism. These findings identify ATF4 as a critical regulator of osteoblast differentiation and function, and indicate that lack of ATF4 phosphorylation by RSK2 may contribute to the skeletal phenotype of CLS.

Results

Decreased Bone Mass in *Rsk2*-Deficient Mice

Based on *Rsk2* expression in osteoblasts and on the existence of skeletal abnormalities in CLS patients, we generated and analyzed *Rsk2*-deficient mice. The mutation engineered was a null allele that did not affect synthesis of other RSKs (Figures 1A–1E). *Rsk2*-deficient mice were born at the expected Mendelian ratio, had a normal lifespan, and no histological or metabolic evi-

*Correspondence: karsenty@bcm.tmc.edu

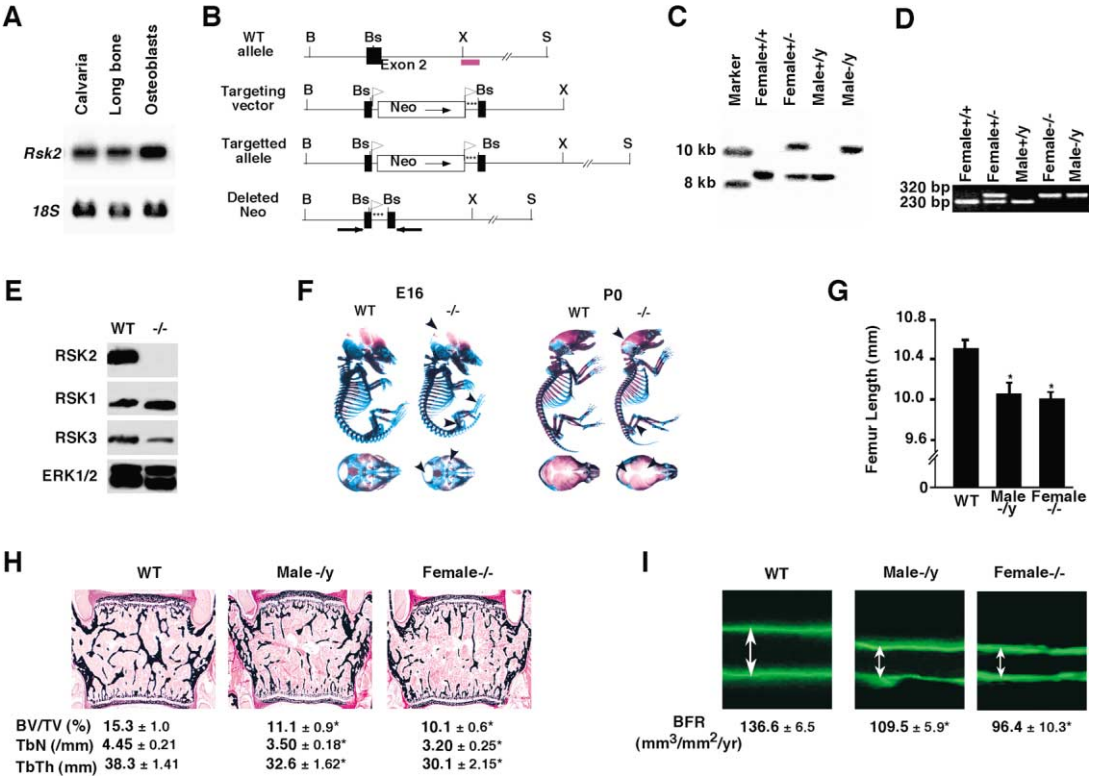

Figure 1. Decreased Bone Mass in *Rsk2*-Deficient Mice

(A) Northern analysis showing *Rsk2* expression in osteoblasts.

(B) Generation of *Rsk2*-deficient mice. Arrows, PCR primers used to distinguish mutant from wild-type (wt) loci; Asterisks, stop codons; Red bar, 3′ external probe; B, BamHI; Bs, BasRI; X, XbaI; and S, SacI.

(C) Southern blot analysis of indicated genotypes using the 3′ external probe. Fragments, wt, 9 kb; mutant, 11 kb.

(D) PCR genotyping. wt and targeted alleles yield 230 bp and 320 bp products, respectively.

(E) Western blot analysis showing absence of RSK2 but presence of RSK1 and RSK3 in *Rsk2*-deficient cells. ERK1/2 was a loading control.

(F) Alizarin red/alcian blue staining of E16 and P0 skeletons. Frontal, parietal, and interparietal bones (arrowheads) are smaller and fontanelles are not closed (bottom) in *Rsk2*-deficient embryos and mice.

(G) Decreased long bone length in *Rsk2*-deficient mice.

(H) Histological analysis of one-month old wt and *Rsk2*-deficient vertebrae. Mineralized bone matrix is stained in black. The ratio of bone volume (BV) versus total tissue volume (TV) is decreased in *Rsk2*-deficient mice.

(I) Calcein double labeling of one-month old wt and *Rsk2*-deficient vertebrae. Bone formation rate (BFR) is decreased in *Rsk2*-deficient mice. Asterisks indicate a statistically significant difference between 2 groups ($p < 0.05$).

dence of internal organs dysfunction (see Supplemental Figure S1 available at http://www.cell.com/cgi/content/full/117/2/387/DC1). Nevertheless, analysis of skeletal preparations stained with alizarin red for mineralized tissue and alcian blue for cartilage revealed that at E16 and at birth *Rsk2*-deficient embryos and pups of either sex had a delay in mineralization of the skull with frontal, parietal, and interparietal bones of reduced size. This resulted in a widening of cranial sutures and opened fontanelles at birth (Figure 1F). *Rsk2*-deficient mice also had a significant reduction in long bone length at one month of age (Figure 1G). These abnormalities are similar to those reported in CLS patients (Young, 1988; Trivier et al., 1996).

Histological analysis revealed that *Rsk2*-deficient mice of either sex had a marked reduction of their bone mass in vertebrae and in long bones at one and two month age (Figure 1H and data not shown). Histomorphometric analysis established that the bone formation rate (BFR), an indicator of osteoblast function, and the number and thickness of trabeculae were markedly decreased in *Rsk2*-deficient mice (Figures 1H and 1I). In contrast, osteoclast number and urinary elimination of deoxypyridinoline, a biochemical marker of osteoclast activity, were both normal in *Rsk2*-deficient mice indicating that bone resorption is not overtly affected in absence of *Rsk2* (data not shown). Together these results reveal the existence of a low bone mass phenotype secondary to a decrease in bone formation in *Rsk2*-deficient mice.

ATF4 Is a Substrate of RSK2 in Osteoblasts

We next asked whether RSK2 phosphorylates transcription factors that may control osteogenesis. Since RSK2 can phosphorylate CREB and c-Fos, two leucine zipper proteins, we used these proteins as positive controls in an in vitro kinase assay and analyzed multiple other leucine zipper proteins as well as Runx2 and Osterix, two transcription factors necessary for osteoblast differentiation (Karsenty and Wagner, 2002). As shown in Fig-

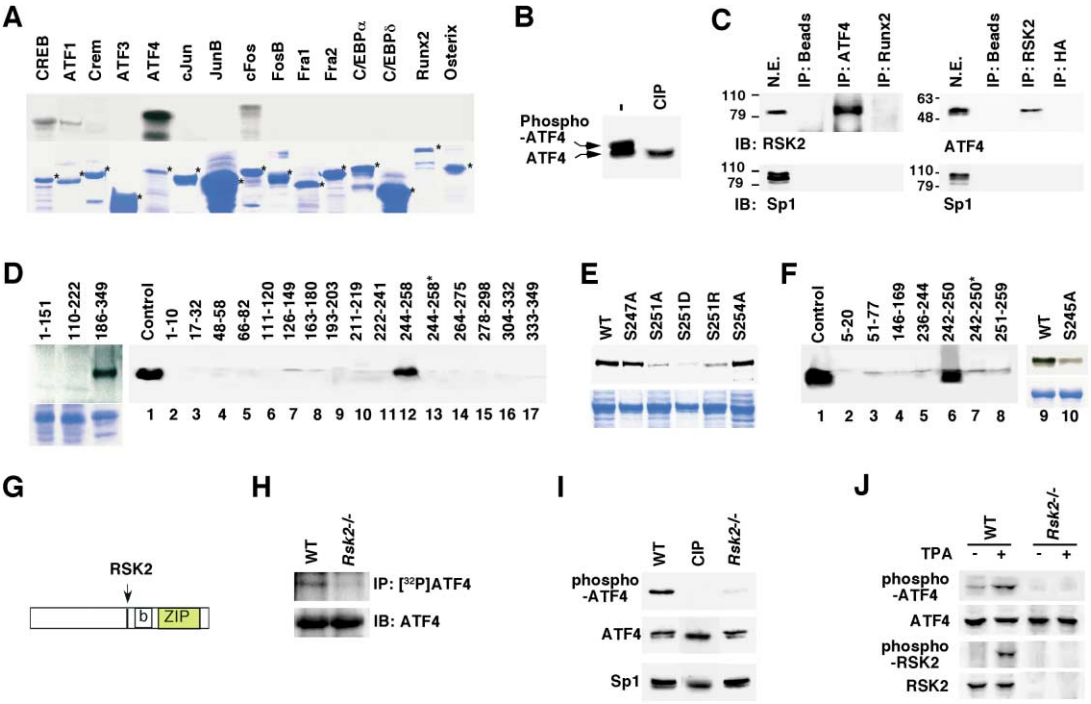

Figure 2. ATF4 Is a Substrate of RSK2 in Osteoblasts

(A) In vitro kinase assays using recombinant proteins. ATF4 is the most heavily phosphorylated protein by RSK2 (top). Asterisks indicate protein input (bottom).

(B) Western blot analysis. ATF4 migrates as a doublet in osteoblast nuclear extracts (NE), the slower migrating band disappears following calf intestinal phosphatase (CIP) treatment.

(C) RSK2 interacts with ATF4 in osteoblasts. Immunoprecipitation of osteoblast NE followed by immunoblotting with either ATF4 or RSK2 antibodies. Controls, NE incubated with Protein G Sepharose alone (beads) or with nonrelated antibodies (anti-Runx2 or anti-HA). SP1 antibody serves as a loading control.

(D) Mapping of RSK2 phosphorylation site in ATF4. ATF4 deletion mutant 186–249 and peptide 244–258 (lane 12) are both phosphorylated by RSK2. Substitution of serine 251 to alanine abolishes this phosphorylation (asterisk, lane 13).

(E) In vitro kinase assays of His-tagged wt ATF4 or mutant ATF4 proteins. Phosphorylation of ATF4-S251A, -251D, or -251R by RSK2 is markedly decreased.

(F) Mapping of RSK2 phosphorylation site to serine 245 in human ATF4. Mutating serine to alanine abolishes phosphorylation in peptide 242–250 (asterisk, lane 7) and in human ATF4.

(G) Location of RSK2 phosphorylation sites in mouse and human ATF4. The basic (b) and leucine zipper (ZIP) domains are boxed.

(H) In vivo phosphorylation of ATF4 is decreased in *Rsk2*-deficient osteoblasts. Probing with an anti-ATF4 antibody indicating the same amounts of ATF4 was used (bottom).

(I) Antiphospho-ATF4 fails to recognize ATF4 following CIP treatment of osteoblast NE (lane 2, top). Phosphorylation of ATF4-S251 is abolished in *Rsk2*-deficient osteoblasts (lane 3, top). ATF4 and Sp1 antibodies were used to monitor protein loading. ATF4 migrates as a doublet as it is phosphorylated by other kinases.

(J) ATF4 phosphorylation in wt but not in *Rsk2*-deficient osteoblasts following TPA treatment. Antiphospho-RSK2 and anti-RSK2 were used as controls (left).

ure 2A, among all proteins tested ATF4 was heavily phosphorylated, while Runx2 and Osterix were not phosphorylated by RSK2. Based on this observation, we investigated the mechanism by which RSK2 may phosphorylate ATF4 in osteoblasts.

In osteoblasts, nuclear extracts ATF4 migrated as a doublet and treatment of nuclear extracts with calf intestinal phosphatase prevented the formation of the slower migrating band indicating that it is a phosphorylated form of ATF4 (Figure 2B). Moreover, an ATF4 antibody precipitated RSK2 present in osteoblast nuclear extracts and conversely a RSK2 antibody precipitated ATF4 thus showing that endogenous RSK2 and ATF4 are able to interact physically (Figure 2C). To identify the amino acid residues in ATF4 phosphorylated by RSK2 we performed in vitro kinase assays using ATF4 deletion mutants and synthetic peptides covering the ATF4 molecule. Only ATF4 deletion mutant encompassing amino acids 186–349 and one internal peptide (244–258) were phosphorylated by RSK2 (Figure 2D). Out of three serine residues contained in this peptide only substitution of serine 251 to alanine, aspartic acid, or arginine nearly abolished ATF4 phosphorylation by RSK2 (Figure 2E). In vitro kinase assay using peptides covering regions of human ATF4 that differs from its mouse-homolog-identified sequence from amino acid 242–250 as being phosphorylated by RSK2 and mutation of serine 245 to alanine decreased phosphorylation of human ATF4 by RSK2 (Figures 2F and 2G) indicating that it is a site of phosphorylation of human ATF4 by RSK2.

To ascertain that RSK2 phosphorylates ATF4 in vivo we used wt and *Rsk2*-deficient osteoblasts. ATF4 immu-

noprecipitation experiments using metabolically labeled wt and *Rsk2*-deficient osteoblast nuclear extracts showed that ^{32}P incorporation into ATF4 was decreased in *Rsk2*-deficient cells (Figure 2H). Furthermore, an ATF4 (S251) phosphospecific antibody reacted with ATF4 in wt but not in *Rsk2*-deficient osteoblasts. The identity of this band as being phosphorylated ATF4 was established by reprobing the same blot with an antibody recognizing all forms of ATF4 (Figure 2I). Lastly, when wt and *Rsk2*-deficient osteoblasts were treated with TPA, an inducer of RSK2 phosphorylation (Merienne et al., 2000), phosphorylation of ATF4 was increased in wt but not in *Rsk2*-deficient osteoblasts (Figure 2J). Taken together, these results support the hypothesis that ATF4 is a target of RSK2 kinase activity in osteoblasts in vivo. This was further tested using several mutant mouse models (see Figure 7).

ATF4 Is Required for Osteoblast Differentiation

The phosphorylation of ATF4 by RSK2 in vivo and the skeletal abnormalities of the *Rsk2*-deficient mice suggested that ATF4 might regulate osteogenesis. That *Atf4*-deficient mice often die perinatally and are runted is compatible with this hypothesis (Tanaka et al., 1998; Hettmann et al., 2000; Masuoka and Townes, 2002). Thus, wt and *Atf4*-deficient embryos and mice were analyzed by skeletal preparations, histology, and osteoblast-specific gene expression.

Alizarin red/alcian blue staining of skeletal preparations of E14 and E16 embryos showed a marked reduction in the area of mineralized tissues in *Atf4*-deficient compared to wt embryos. This defect was observed in frontal and parietal bones, two bones also affected by *Rsk2* deletion (see Figure 1), and in clavicles and long bones. At birth, the delay of mineralization in the skull was still present as shown by widening of the fontanelles (Figure 3A). At all stages analyzed, $Atf4^{+/-}$ mice looked indistinguishable from wt littermates (data not shown).

Histological analysis revealed no difference between wt and *Atf4*-deficient skeletal elements in E13 or younger embryos indicating that ATF4 was dispensable for early stages of skeletogenesis (Supplemental Figure S2 available on *Cell* website). In contrast, a noticeable delay in osteoblast differentiation was observed throughout the skeleton in E15 *Atf4*-deficient embryos. For instance, trabeculae were absent in *Atf4*-deficient frontal bones while they were already present in wt skulls. In E16, *Atf4*-deficient skulls trabeculae were short, thin, and rare while in wt skulls they were long, thick, and numerous. At birth, trabeculae in *Atf4*-deficient skulls remained strikingly thinner than in wt skulls (Figure 3B, a, b, e, f, i, and j). This peculiar thinning of trabeculae provides a plausible explanation for the perinatal lethality of *Atf4*-deficient mice as the brain is poorly protected during delivery. The same delay in appearance of bone existed in *Atf4*-deficient appendicular skeleton. In E15, wt embryos a bone collar surrounding the future long bones was visible and trabeculae were present, in contrast there was no morphological evidence of trabeculae or of a bone collar in E15 *Atf4*-deficient long bones. In E16, wt long bones numerous trabeculae were present while none could be found in *Atf4*-deficient long bones. At birth there were some trabeculae in *Atf4*-deficient long bones while they remained rare, short, and markedly thinner compared to wt ones (Figure 3B, m, n, q, r, u, and v).

There was also molecular evidence of a delay in osteoblast differentiation in absence of *Atf4*. For instance, expression of *Bone Sialoprotein* (*Bsp*), a molecular marker of differentiated osteoblasts (Aubin and Triffitt, 2002), was undetectable in E15 and E16 *Atf4*-deficient skulls and long bones and much weaker in newborn *Atf4*-deficient skulls (Figure 3B, c, d, g, h, k, l, o, p, s, t, w, and x). Likewise, expression of *Osteocalcin*, the latest marker of differentiated osteoblasts to appear (Aubin and Triffitt, 2002), was decreased in E16 *Atf4*-deficient embryos and newborn mice compared to wt littermates (Figure 3C, a–d). In contrast, expression of genes characteristic of earlier stages of osteoblast differentiation was not affected by *Atf4* inactivation. Indeed, *Runx2* and *Osterix* (Figure 3C, e–l), two transcription factors required for differentiation of mesenchymal cells into osteoblasts, and α*1(I) Collagen* (Figure 3C, m–p), were all normally expressed in absence of *Atf4*. Together, these histological and molecular observations demonstrate that ATF4 is required for the timely onset and for terminal differentiation of osteoblasts.

To ascertain that *Atf4* expression was compatible with its role during skeletal development, we studied its expression in E16 wt embryos. Consistent with its function during fetal liver hematopoiesis, *Atf4* was highly expressed in liver; however, skeleton was the second highest site of *Atf4* expression. In the skeleton, *Atf4* expression was present in osteoblasts and was markedly reduced in cells occupying E16 *Runx2*-deficient skeletal elements indicating that *Atf4* expression in osteoblasts is dependent on *Runx2* expression (Figures 3D and 3E). Consistent with this hypothesis there is a bona fide Runx2 binding site in the *Atf4* promoter (Figures 3F and 3G).

Osteocalcin Is a Target Gene of ATF4 In Vivo

The decreased *Osteocalcin* expression in *Atf4*-deficient embryos suggested that this gene may be a target of ATF4. Two osteoblast-specific *cis*-acting elements are present in the *Osteocalcin* promoter (Ducy and Karsenty, 1995). One of them is the binding site for Runx2 while OSE1, binds an osteoblast-specific nuclear protein that has been partially purified (Schinke and Karsenty, 1999) (Figure 4A). Several lines of evidence indicate that this OSE1 binding protein and ATF4 are indistinguishable.

First, OSE1 sequence has homology with a CREB/ATF binding site and purified OSE1 binding protein still bound DNA after boiling (Figures 4A and 4B), a hallmark of leucine zipper-containing transcription factors (McKnight, 1992). Second, ATF4 bound to wt OSE1 but not to mutated forms of OSE1 to which OSE1 binding protein could not bind either and no other leucine zipper proteins tested had the same binding profile (Figure 4C). Third, only antibodies directed against ATF4 could supershift or inhibit binding of osteoblast nuclear extracts to OSE1 (Figure 4D and Supplemental Figure S3A available on *Cell* website). Fourth, the OSE1 binding activity present in wt nuclear extracts was absent in *Atf4*-deficient osteoblast nuclear extracts (Figure 4E). Fifth, in chromatin immunoprecipitation (ChIP) assay an

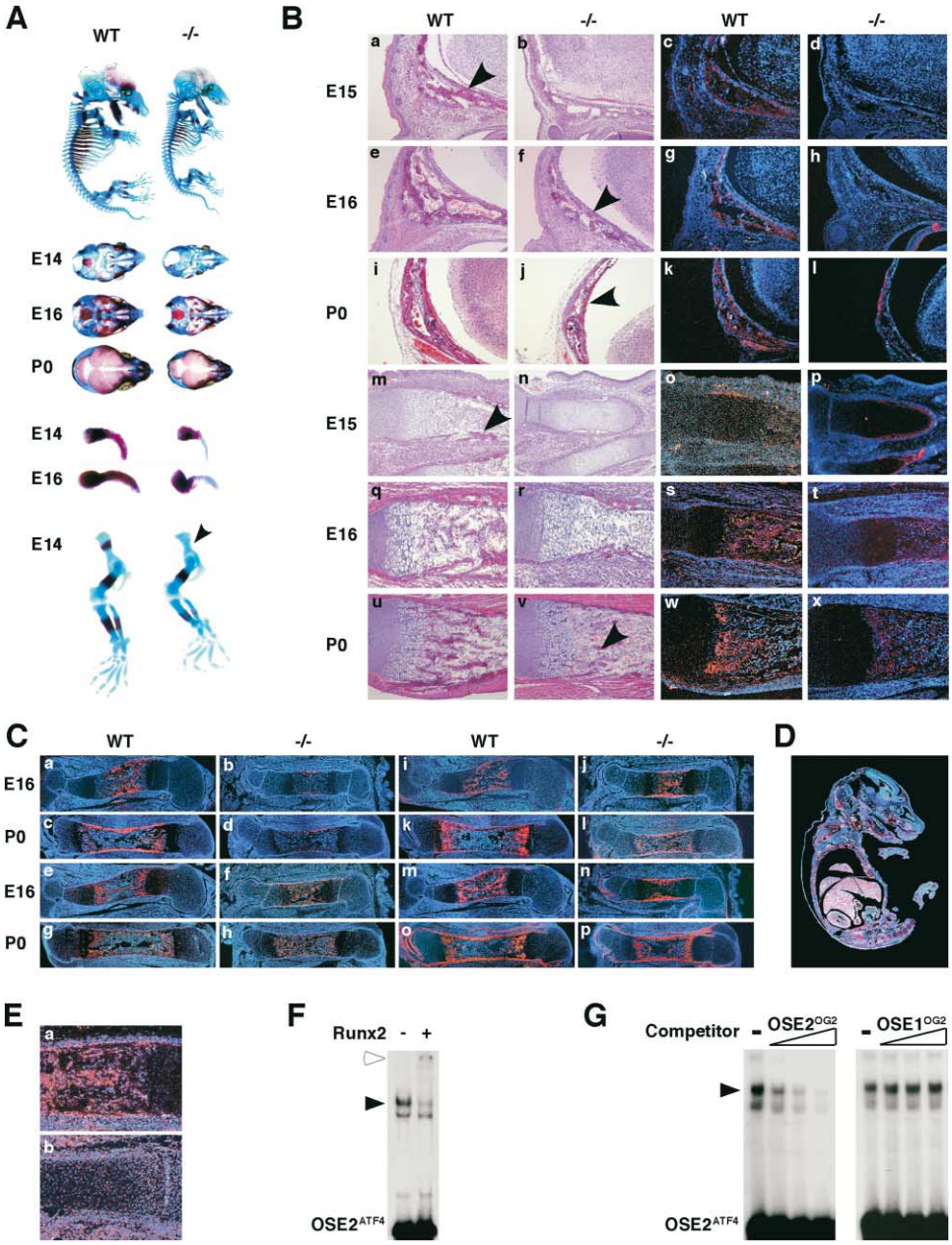

Figure 3. Delayed Skeletal Development in Absence of *Atf4*

(A) Alcian blue/alizarin red staining of E14, E16, and P0 wt and *Atf4*-deficient skeletons. Note the lack of alizarin red staining in skull, clavicles (E14 and E16), and limbs (E14) in *Atf4*-deficient embryos and the widening of fontanelles in *Atf4*-deficient newborn mice (arrowhead).

(B) H&E staining of wt (a, e, i, m, q, and u) and *Atf4*-deficient (b, f, j, n, r, and v) embryos and mice at E15 (a, b, m, and n), E16 (e, f, q, and r) and P0 (i, j, u, and v). Note the delay in bone formation in *Atf4*-deficient skulls (a, b, e, f, i, and j) and long bones (m, n, q, r, u, and v) at all stages. In situ hybridization of wt (c, g, k, o, s, and w) and *Atf4*-deficient (d, h, l, p, t, and x) skulls (c, d, g, h, k, and l) and limbs (o, p, s, t, w, and x) using *Bsp* as a probe. *Bsp* expression is absent in E15 and E16 *Atf4*-deficient skulls and markedly reduced in P0 *Atf4*-deficient skulls. It is also decreased in *Atf4*-deficient limbs compared to wt controls at all time points analyzed. Magnification: 100×.

(C) In situ hybridization analysis of wt (a, c, e, g, i, k, m, and o) and *Atf4*-deficient long bones (b, d, f, h, j, l, n, and p), E16 (a, b, e, f, i, j, m, and n) embryos, and P0 mice (c, d, g, h, k, l, o, and p). Probes are: *Osteocalcin* (a–d), *Runx2* (e–h), *Osterix* (i–l), and *a1(I) Collagen* (m–p). Only *Osteocalcin* expression is decreased in *Atf4*-deficient bones at all stages analyzed. Magnification: 50×.

(D) *Atf4* expression in skeleton of E16 wt embryos. Magnification: 25×.

(E) *Atf4* expression is reduced in E16 *Runx2*-deficient bones (b) compared to wt (a) littermates. Magnification: 100×.

(F) Electrophoresis mobility shift assay (EMSA). Runx2 binds to an OSE2 site present in *Atf4* promoter (OSE^{ATF4}, solid arrowhead). Runx2 antibody supershifts this protein-DNA complex (empty arrowhead).

(G) EMSA. Increasing amount of specific ($OSE2^{OG2}$) but not of nonspecific ($OSE1^{OG2}$) cold competitors at 0, 50×, 100×, and 200× excess of radiolabeled probe (triangles) inhibits binding of Runx2 to $OSE2^{ATF4}$.

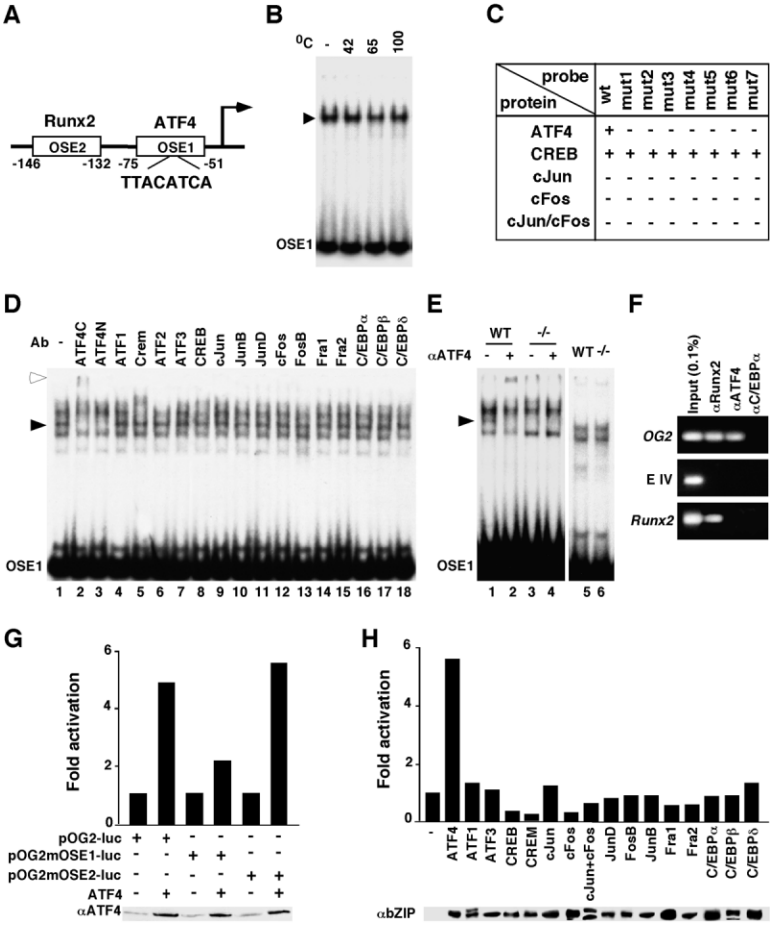

Figure 4. *Osteocalcin* Is a Target Gene of ATF4

(A) *Osteocalcin* promoter (OG2) showing OSE2 (Runx2 binding site) and OSE1 (ATF4 binding site).

(B) EMSA. Purified OSE1 binding protein still binds to OSE1 after boiling.

(C) Binding of indicated leucine zipper proteins to wt or mutant OSE1 oligonucleotides. Only ATF4 behaves like OSE1 binding protein.

(D) Only ATF4 antibodies supershifted (empty arrowhead, lane 2) or prevented formation (solid arrowhead, lane 3) of nuclear extracts-OSE1 complex.

(E) EMSA. Absence of binding activity to OSE1 in *Atf4*-deficient osteoblast nuclear extracts. Runx2 binding to OSE2 (lanes 5 and 6) was used as a control of nuclear extract quality.

(F) ChIP analysis. ATF4 binds to the *Osteocalcin* promoter (*OG2*) but not to its coding region (E IV) or to the Runx2 promoter (*Runx2*). Runx2 and C/EBPα antibodies were used as positive and negative controls, respectively (Ducy et al., 1999).

(G) DNA cotransfection using wt or mutant pOG2-luc reporter and expression vectors of ATF4 and indicated proteins in COS cells. Fold activations are shown. Western blot (bottom) shows the presence of ATF4 in transfected cells.

(H) DNA cotransfection assays showing specificity of ATF4 function. Western blot (bottom) verified expression of proteins tested.

ATF4 antibody precipitated the *Osteocalcin* promoter, as did an antibody against Runx2, a known regulator of *Osteocalcin* (Ducy et al., 1997). These immunoprecipitations were specific since ATF4 antibody could not precipitate *Osteocalcin* coding region or an unrelated promoter (*Runx2* promoter). Moreover, an antibody against another leucine zipper protein failed to precipitate this *Osteocalcin* promoter fragment (Figure 4F). Lastly, in DNA cotransfection experiments, an *Atf4* expression vector increased activity of an *Osteocalcin* promoter-luciferase chimeric gene (pOG2-luc) 5-fold. A mutation abolishing Runx2 binding to OSE2 in this promoter fragment did not affect ATF4 transactivation ability while a mutation eliminating binding of nuclear proteins to OSE1 did (Figure 4G). Again, none of the leucine zipper proteins tested, even members of the CREB family, transactivated pOG2-luc (Figure 4H and Supplemental Figure S3B available on *Cell* website). These findings along with the decrease in *Osteocalcin* expression observed in *Atf4*-deficient mice indicate that *Osteocalcin* is a target gene of ATF4 in vivo.

ATF4 Controls Bone Mass Postnatally

That a significant number of *Atf4*-deficient mice lived beyond birth allowed us also to determine whether ATF4 is required for bone homeostasis postnatally. Histological analysis at multiple time points over a year showed a severe reduction in bone volume and in the number and thickness of trabeculae in *Atf4*-deficient bones. As a result *Atf4*-deficient mice failed to ever reach a normal bone mass indicating that ATF4 is required for bone mass accrual (Figures 5A and 5B). This phenotype was due in part to a failure to achieve terminal differentiation of osteoblasts as shown by the 2-fold decrease in *Osteocalcin* expression in *Atf4*-deficient bones (Figure 5C). This was also due to a defect in osteoblast function as shown by a 2-fold decrease in the rate of bone formation in adult *Atf4*-deficient bones (Figure 5D). Thus, the bone phenotype of adult *Atf4*-deficient mice is similar to the one observed in *Rsk2*-deficient mice. *Atf4*-deficient mice bone phenotype was also reminiscent of the one seen in mice lacking LRP5 (Kato et al., 2002), however, ATF4 was present in *Lrp5*-deficient osteoblast nuclear extracts (Supplemental Figure S4 available on *Cell* website).

Decrease Type I Collagen Synthesis in Absence of ATF4

Bone trabeculae were abnormally thin in absence of *Atf4* and *Atf4*-deficient osteoblasts were considerably smaller than wt osteoblasts (Figure 6A). This small cell size was not observed in bone marrow cells or in osteoclasts indicating that *Atf4* inactivation did not cause a general defect of cell size (Figures 6A and 6B). This raised the hypothesis that a defect in protein synthesis may exist in *Atf4*-deficient osteoblasts. To test this hy-

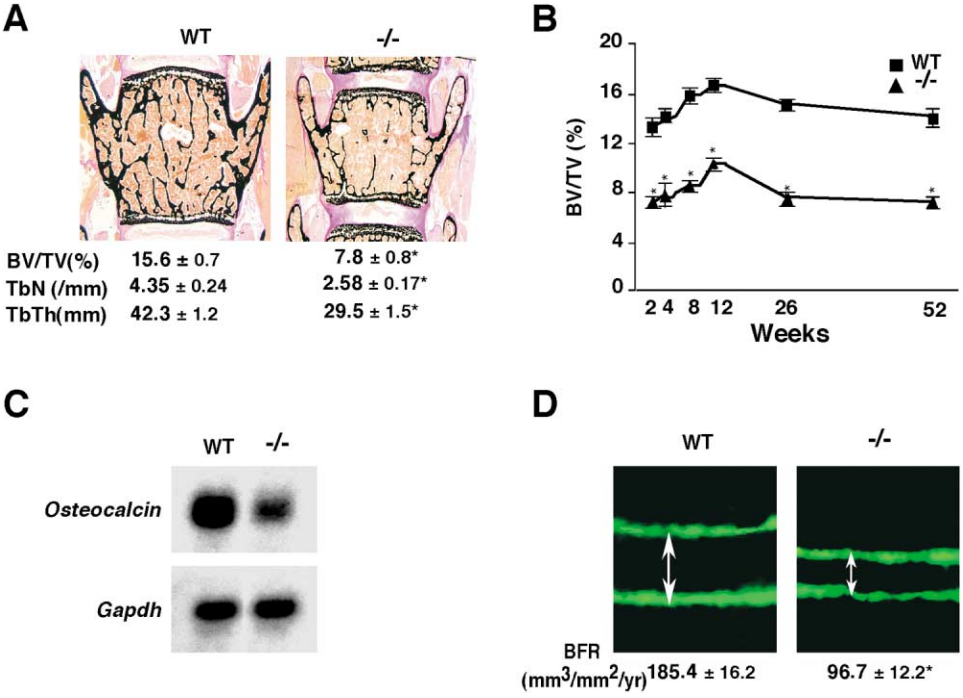

Figure 5. Low Bone Mass in *Atf4*-Deficient Mice

(A) Histomorphometric analysis of two-month-old wt and *Atf4*-deficient vertebrae. Note the decrease in bone volume (BV/TV), trabeculae number (TbN), and trabecular thickness (TbTh) in *Atf4*-deficient mice.

(B) *Atf4*-deficient mice fail to acquire a normal bone mass postnatally.

(C) Decreased *Osteocalcin* expression in *Atf4*-deficient bones.

(D) Decreased BFR in two-month-old *Atf4*-deficient mice.

pothesis, we examined synthesis of Type I collagen, the main biosynthetic product of osteoblasts, in wt and *Atf4*-deficient osteoblasts.

Using van Gieson reagent, which stains specifically collagen fibrils, we noticed a dramatic decrease of collagen content in E16 *Atf4*-deficient compared to wt or heterozygous tibia (Figure 6C). When cultured in absence of nonessential amino acids, Type I collagen syn-

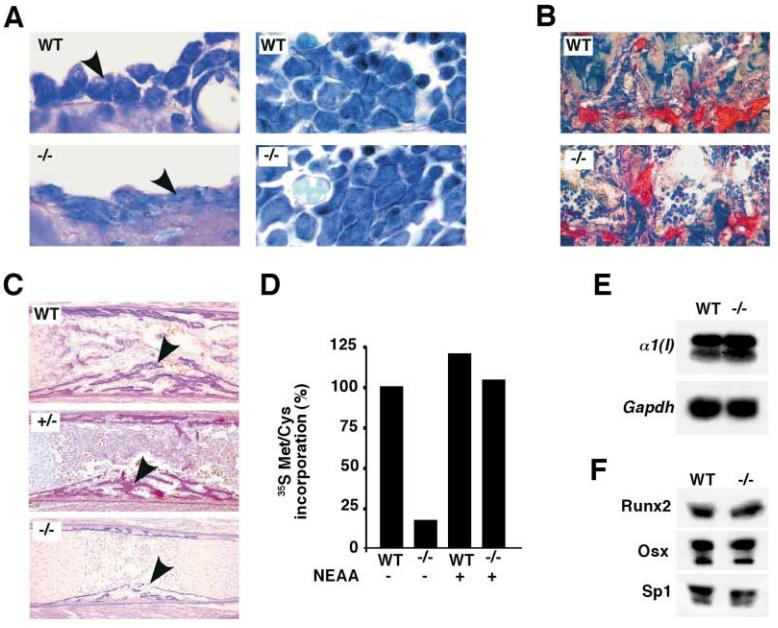

Figure 6. ATF4 Is Required for Type I Collagen Synthesis in Osteoblasts

(A) Toluidine blue staining of one-month-old vertebrae. *Atf4*-deficient osteoblasts are smaller than wt (arrowheads) whereas bone marrow cells are of similar size (400×).

(B) TRAP-staining of one-month-old vertebrae. Osteoclast size is similar in *Atf4*-deficient bones (400×).

(C) van Gieson staining of wt, $Atf4^{+/-}$, and $Atf4^{-/-}$ E16 tibia. Reduced number of van Gieson-stained collagen-rich trabeculae in *Atf4*-deficient tibia (arrowheads). Magnification: 100×.

(D) Type I collagen synthesis analysis. Synthesis of both α1 and α2 chains of Type I collagen are decreased in *Atf4*-deficient osteoblasts; addition of nonessential amino acids (NEAA) to cultures rescues this defect. Histogram shows the percentage of ^{35}S-Methionine/Cystein incorporation into both α1 and α2 chains of Type I collagen relative to β-actin control (n = 3).

(E) Normal *α1(I) Collagen* expression in *Atf4*-deficient osteoblasts.

(F) Normal abundance of Runx2 and Osterix in *Atf4*-deficient osteoblasts. Sp1 serves as a loading control.

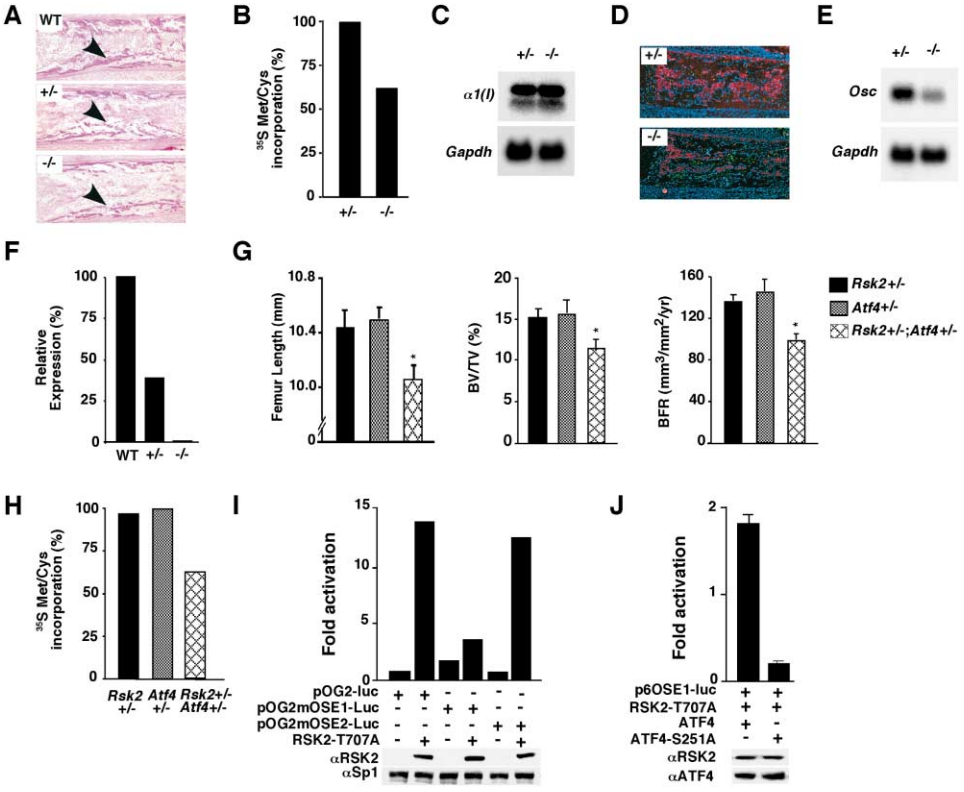

Figure 7. Genetic Interaction between RSK2 and ATF4

(A) van Gieson staining of E16 female wt, *Rsk2*$^{+/-}$ and *Rsk2*$^{-/-}$ tibia showing decreased collagen content only in *Rsk2*$^{-/-}$ limbs (100×).

(B) Decreased Type I collagen synthesis in *Rsk2*-deficient osteoblasts.

(C) Normal expression of α*1(I) Collagen* in *Rsk2*-deficient osteoblasts.

(D) Decreased expression of *Bsp* in E16 *Rsk2*-deficient bones.

(E) Decreased expression of *Osteocalcin* in *Rsk2*-deficient osteoblasts.

(F) Expression of wt *Rsk2* allele in heterozygous mutant mice by real-time reverse transcriptase-PCR.

(G) Decreased long bone length (left), bone mass (middle) and bone formation rate (right) in 1-month *Atf4*$^{+/-}$; *Rsk2*$^{+/-}$ female mice.

(H) Decreased Type I collagen synthesis in *Atf4*$^{+/-}$; *Rsk2*$^{+/-}$ osteoblasts.

(I) RSK2 increases OG2 promoter activity through OSE1. RSK2 expression was confirmed by Western blot. Sp1 serves as a loading control (bottom).

(J) RSK2 enhances ATF4 transcriptional ability. DNA cotransfection assays using p6OSE1-Luc as a reporter vector (200 ng) and RSK2-T707A (10 ng), ATF4 (25 ng) or ATF4-S251A (25 ng) as expression vectors. RSK2-T707A doubled the transactivation activity of wt ATF4 but not of ATF4-S251A. Western blot verified the presence of RSK2 and ATF4 proteins.

thesis was decreased 7–10-fold in *Atf4*-deficient but not in wt osteoblasts. Addition of nonessential amino acids in culture medium corrected the defect in collagen synthesis in osteoblasts lacking ATF4 (Figure 6D). This decrease in Type I collagen synthesis was not due to a decrease of gene expression as α*1(I) Collagen* expression was identical in wt and mutant osteoblasts (Figure 6E). Likewise, Runx2 and Osterix were present in normal abundance in *Atf4*-deficient osteoblasts (Figure 6F). This result indicates that the decrease in Type I collagen synthesis observed in *Atf4*-deficient osteoblasts is secondary to a decrease in amino acid import, a function regulated by ATF4 in other cell types (Harding et al., 2003). It also establishes that part of the skeletal phenotype observed in absence of *Atf4* can be attributed to a posttranscriptional defect.

RSK2 Interacts with and Modulates Transactivation Function of ATF4

The similarity in the bone phenotypes caused by either *Rsk2* or *Atf4* inactivation and the lack of phosphorylation of ATF4 in *Rsk2*-deficient osteoblasts implied that RSK2 and ATF4 act in a linear cascade controlling osteoblast differentiation and function. If this is the case, cellular and molecular abnormalities present in *Atf4*-deficient mice should be present in *Rsk2*-deficient mice. Additionally *Rsk2*$^{+/-}$; *Atf4*$^{+/-}$ mice may have phenotypic and cellular abnormalities similar to the ones seen in *Rsk2*- and *Atf4*-deficient mice.

To test the first hypothesis, we measured Type I collagen synthesis in *Rsk2*-deficient female mice as posttranscriptional decrease of Type I collagen synthesis is a characteristic feature of *Atf4*-deficient mice. As shown in Figure 1H, trabeculae were thinner and van Gieson staining showed a marked decrease in collagen abundance in bones lacking *Rsk2* (Figure 7A). Consistent with this histological finding, Type I collagen synthesis was decreased in *Rsk2*-deficient osteoblasts while α*(I) collagen* expression was not (Figures 7B and 7C). This posttranscriptional alteration of Type I collagen synthesis linked together the phenotypes of *Rsk2*- and of *Atf4*-deficient mice and also showed that the defect in *Rsk2*-deficient

osteoblasts was, at least in part, cell autonomous. In addition, *Bsp* and *Osteocalcin,* two genes whose expression was decreased in *Atf4*-deficient embryos and osteoblasts, were also expressed at low levels in *Rsk2*-deficient bones and osteoblasts, respectively (Figures 7D and 7E). To test the second hypothesis, we generated female mice lacking one copy of *Atf4* and one copy of *Rsk2* and analyzed them at one month of age. Since *Rsk2* does not escape X-inactivation, $Rsk2^{+/-}$ female mice are mosaic and express also the wt allele (Figure 7F). $Rsk2^{+/-}$; $Atf4^{+/-}$ mice had shorter long bones and histological analysis showed a lower bone mass and decreased bone formation rate compared to single heterozygous littermates (Figure 7G). Type I collagen production was also decreased in $Rsk2^{+/-}$; $Atf4^{+/-}$ osteoblasts but its expression was not (Figure 7H).

Taken together, the histological features, gene expression abnormalities, and the decrease of Type I collagen production shared by *Rsk2*-deficient, *Atf4*-deficient, and $Rsk2^{+/-}$; $Atf4^{+/-}$ mice corroborate the lack of ATF4 phosphorylation in *Rsk2*-deficient osteoblasts presented in Figure 2 and support the hypothesis that RSK2 and ATF4 act in a cascade to control osteoblast differentiation and function.

The identification of *Osteocalcin* as an ATF4 target gene in osteoblasts allowed us to ask whether phosphorylation by RSK2 affects ATF4's transactivation ability. Forced expression of a constitutively active form of RSK2 (RSK2-T707A) (Poteet-Smith et al., 1999) in COS cells increased the activity of pOG2-luc reporter (Figure 7I). This effect of RSK2-T707A required an intact OSE1 element, suggesting that phosphorylation of ATF4 by RSK2 enhances its transactivation ability. Consistent with this hypothesis RSK2-T707A nearly doubled the transactivation ability of wt ATF4 when using a reporter construct containing six copies of OSE1 (p6OSE1-Luc); in contrast RSK2-T707A could not increase the activity of ATF4-S251A, an ATF4 mutant that cannot be phosphorylated by RSK2 (Figure 7J).

Discussion

This study reveals that ATF4 is a major regulator of osteoblast differentiation. ATF4 also affects, through a posttranscriptional mechanism, synthesis of Type I collagen, the main function of osteoblasts. The regulation of osteoblast function by ATF4 indicates that besides determining factors such as Runx2 other transcription factors are required for maintenance of the osteoblast phenotype. Furthermore, by showing that phosphorylation by RSK2 affects ATF4 functions this study also suggests a molecular explanation for the skeletal manifestations observed in CLS.

Cellular and Molecular Bases of RSK2 Function in Osteoblasts

The initial descriptions of CLS reported skeletal abnormalities including short stature, delayed bone age, delayed closure of fontanelles, osteopenia, and digital dysmorphism (Coffin et al., 1966; Lowry et al., 1971; Temtamy et al., 1975). We show here using *Rsk2*-deficient mice that these abnormalities are due to a defect in osteoblast function. Based on in vitro kinase assays several substrates have been proposed for RSK2 including CREB, c-Fos, and estrogen receptor (ERα) (Xing et al., 1996; De Cesare et al., 1998; Joel et al., 1998; Bruning et al., 2000). However, *c-Fos* or *Er*α inactivation in mice do not cause a bone phenotype similar to the one observed in *Rsk2*-deficient mice (Johnson et al., 1992; Wang et al., 1992; Sims et al., 2002). Our in vitro kinase assay identifies ATF4 as an additional target of RSK2. ATF4 and RSK2 interact physically and serines 251 and 245 in mouse and human ATF4 respectively are phosphorylated by RSK2. Several lines of evidence support the contention that ATF4 is a substrate of RSK2 in osteoblasts in vivo. First, ^{32}P incorporation into ATF4 is reduced in *Rsk2*-deficient cells; second, a phosphoantibody directed toward serine 251 failed to detect ATF4 in *Rsk2*-deficient osteoblasts; third, the same cellular (decrease in Type I collagen synthesis) and molecular (decrease in *BSP* and *Osteocalcin* expression) abnormalities are present in *Rsk2*- and *Atf4*-deficient mice; fourth, $Rsk2^{+/-}$; $Atf4^{+/-}$ mice have low bone mass phenotype similar to the one of *Rsk2*-deficient mice.

DNA cotransfection assays showed that RSK2 phosphorylation modulates ATF4 transactivation function. Indeed, a constitutively active form of RSK2 increased *Osteocalcin* promoter activity through an ATF4 binding site. Additionally, this constitutively active form of RSK2 enhanced the transcription function of wt ATF4 but not of ATF4-S251A that cannot be phosphorylated by RSK2. *Atf4*-deficient mice have a much more severe skeletal phenotype than *Rsk2*-deficient mice suggesting ATF4's function is regulated by other modifications. This hypothesis is consistent with the existence of multiple phosphorylation sites in ATF4. Our results do not exclude the possibility that other transcription factor(s) may also serve as RSK2 substrate(s) in osteoblasts nor do we rule out either that RSK2 may have other substrates in other organs such as brain where its inactivation causes major phenotypic abnormalities.

ATF4 and Osteoblast Biology

ATF4 affects all aspects of osteoblast biology. In absence of ATF4, the appearance of bone trabeculae is delayed. This delay in osteogenesis suggests that ATF4 is required to mediate some aspects of Runx2 osteoblast differentiation function. The near abolition of *Atf4* expression in *Runx2*-deficient bone and the presence of a Runx2 binding site in *Atf4* promoter are consistent with this hypothesis that can now be tested in vivo. However, the observation that bone formation occurs, albeit in a delayed and abnormal manner, in absence of ATF4 indicates that ATF4 is at least partially dispensable for differentiation of mesenchymal cells into osteoblasts.

In contrast ATF4 plays a more permanent role in osteoblast terminal differentiation. In situ and Northern blot analyses showed that in *Atf4*-deficient osteoblasts *Bsp* and *Osteocalcin* expression were markedly reduced during development and after birth. The identification of *Osteocalcin* as an ATF4 target gene in osteoblasts establishes that some ATF4 functions occur through a transcriptional mechanism. It will be important now to identify other ATF4 target gene(s) regulating osteoblast differentiation to decipher how bone mass accrual is determined postnatally.

ATF4 Control of Bone Formation and Amino Acid Import

ATF4 also controls bone formation through a posttranscriptional mechanism by regulating the most important function of osteoblasts: their ability to synthesize Type I collagen, a protein accounting for 90% of the bone ECM protein content (Prockop and Kivirikko, 1995). This function of ATF4 is critical to explain the virtual absence of bone trabeculae before and after birth in *Atf4*-deficient mice.

Multiple lines of evidence established in recent years that ATF4 is an integral component of the pathway controlling amino acid import that protects against oxidative stress. This pathway is initiated by phosphorylation of eukaryotic translation initiation factor 2 (eIF2α) and expression of *Atf4* is dependent on eIF2α phosphorylation (Harding et al., 2002). PERK is one kinase that phosphorylates eIF2α. Interestingly mice and human deficient in PERK have the same abnormal thinning of bone trabeculae as the one observed in *Atf4*-deficient mice (Delepine et al., 2000; Harding et al., 2000; Zhang et al., 2002). However, PERK deficiency affects other secretory cells leading for instance to exocrine and endocrine pancreas failure (Harding et al., 2001). That this is not the case in *Atf4*-deficient mice reveals a functional specificity of ATF4 in osteoblasts.

Determining and Maintenance Factors in Osteoblast Biology

A notion emerging from this and other studies is that there are two types of regulatory molecules at work in osteoblasts. The first group comprises determining factors (Runx2 and Osterix) that are necessary and/or sufficient for the differentiation of osteochondroprogenitor cells into osteoblasts. To date, the thrust of their function appeared to be at this initial stage of differentiation. A second group of molecules includes LRP5 (Gong et al., 2001; Kato et al., 2002) and ATF4. These molecules are required to maintain the normal phenotype of osteoblasts including their ability to synthesize bone ECM proteins. Although this distinction may not be absolute, it provides a useful molecular framework to understand how osteoblast differentiation and ultimately function is controlled in vertebrates. This should also be useful to uncover genetic pathways linking osteoblast differentiation and osteoblast function.

Experimental Procedures

Mutant Mice

Rsk2-deficient mice were generated using a targeting vector containing a neomycin resistant (*Neo*^{R}) gene and 3 stop codons in three different frames at the end of the coding sequence inserted into exon 2. Additionally, one loxP site at either ends of *Neo*^{R} (see Figure 1B) was present. The *Neo*^{R} was flanked by a 2 kb and 9 kb *Rsk2* genomic DNA at its 5′ and 3′ end, respectively. The linearized construct was electroporated into 129SvJ embryonic stem (ES) cells, targeted ES cell clones identified by Southern blot were injected into C57BL/6J blastocysts. *Neo*^{R} was removed by crossing mutant mice with CMV-Cre transgenic mice. Primer sequences used for genotyping of *Rsk2*-deficient mice are available upon request. Generation of *Atf4*-deficient mice has been described (Masuoka and Townes, 2002). Six to twelve animals of each genotype were analyzed for all studies, statistical significance was assessed by Student's t test. Error bars represent standard errors of the means (SEM).

Morphological Analysis

Alcian blue/alizarin red staining of skeletal preparations were performed using standard protocols (McLeod, 1980). For histological analysis, skeletons were fixed in 4% paraformaldehyde (PFA). Mice were injected with calcein at six and two days prior to sacrifice. Lumbar vertebrae sections (7 μm) were stained with van Gieson and von Kossa reagents. Histomorphometric analysis was performed using the OsteoMeasure Analysis System (Osteometrics, Inc.) according to standard criteria (Parfitt et al., 1987). Alternate sections stained with 1% toluidine blue were used for quantifying osteoblast numbers.

Gene Expression

For Northern blot analysis, total RNA of indicated sources were extracted with Trizol (Invitrogen) and hybridized with appropriate probes. *Gapdh* or *18S* were used as a loading control. For in situ hybridization analyses, embryos and pups were fixed in 4% PFA, embedded in parafilm, and sectioned at 5 μm. A 271 bp 5′ untranslated region of *Atf4* and a 390 bp 5′ untranslated and partial of coding region of *Osterix* were cloned by RT-PCR and used to generate [^{35}S]-labeled antisense riboprobes, other probes have been described (Ducy et al., 1997). Nuclear extracts (NE) of calvarial osteoblasts or ROS17/2.8 cells were incubated with labeled OSE1 probe at room temperature (RT) for 5 min. All antibodies tested were purchased from Santa Cruz except ATF4-N which was raised against epitope QETNKEPPQTVNPIGHLPES. ChIP was performed according to manufacturer's instruction (Upstate) using primary osteoblasts of indicated genotypes. PCR primer sequences are available upon request. COS cells were plated at 5 $\times$ 10^4/well in 12-well plates and transfected with 0.5 μg of pOG2-luc and 0.05 μg of RSV-β-gal reporter vectors together with 0.5 μg of each expression plasmids unless otherwise indicated. Luciferase and β-galactosidase assays were performed using standard procedures. Data represent ratios of luciferase/β-galactosidase activity.

Protein Chemistry

NE (500 μg) from calvarial osteoblasts or ROS 17/2.8 osteoblastic cells were diluted with RIPA buffer (50 mM Tris-Cl, [pH 7.6], 150 mM NaCl, 1% NP-40, 0.5% Na-deoxycholate, and 0.1% SDS) and incubated at 4°C for 1 hr (h) with RSK2 or ATF4 antibody (Santa Cruz) in the presence of protease inhibitors. Protein G Sepharose (20 μl) (Amersham Pharmacia) was added for another hour. Sepharose beads were washed four times and precipitated proteins resolved by 10% SDS-PAGE followed by Western blot using ATF4 and RSK2 antibodies. Total nuclear proteins (25 μg) were treated with 20 U of calf intestine alkaline phosphatase (Amersham Pharmacia) at RT for 30 min, separated on a 10% SDS-PAGE followed by Western blot analysis using anti-ATF4 antibody. In vitro kinase assays using active forms of mouse RSK2 (Upstate) were performed as follows. GST or His-tagged recombinant proteins were expressed in bacteria and purified according to standard protocols. Kinase reactions were performed at RT for ten min in the presence of [^{33}P]-γATP, phosphorylated products were resolved on a 10% SDS-PAGE before detection by autoradiography. Mutagenesis of ATF4 was performed using a mutagenesis kit (Stratagene) following the manufacturer's instructions. Integrity of all constructs was confirmed by DNA sequencing. Phospho-ATF4 antibody was generated against synthetic peptide NLPSPGGSRGSPPK in which the underlined serine was phosphorylated. Primary osteoblasts were labeled with 1 mCi/ml [^{32}P]-orthophosphate (Perkin Elmer) for eight hr in DMEM (phosphate free; Invitrogen) supplemented with 10% dialyzed FBS. ATF4 was immunoprecipitated using equal number of cpm for wt or *Rsk2*-deficient NE, separated by SDS-PAGE, membrane transferred, and visualized by autoradiography. Prior to 12-o-tetradecanoyl phorbol-13-acetate (TPA) treatment, 90% confluent wt, and *Rsk2*-deficient osteoblasts were grown in α-MEM containing 0.1% FCS 16 hr, TPA was added for 15 min. For collagen synthesis wt, *Atf4*-, and *Rsk2*-deficient osteoblasts were labeled with 50 μCi/ml of [^{35}S] methionine and cysteine mix (Amersham Pharmacia) for 12 hr in DMEM (methionine and cysteine free; Invitrogen) supplemented with 2% dialyzed FBS, 2 mM L-glutamine, 55 μM β-mercaptoethanol, with or without nonessential amino acid mix. Cells were homogenized, procollagen digested to collagen with 50 μg/ml of pepsin, and Type I collagen

precipitated (0.7 M NaCl), and resolved by 7% SDS-PAGE containing 2 M urea as described (Bonadio et al., 1985).

Acknowledgments

We thank D. Ron and E. Wagner for sharing information prior to publication and for critical reading of the manuscript; G. Darlington, B. De Crombrugghe, E. Wagner, and T. Strugill for reagents; and P. Ducy and F. Ramirez for suggestions on the manuscript. This work was supported by grants from the National Institute of Health (G.K.) and Human Frontier Organization and the Association pour la Recherche sur le Cancer (A.H.), fellowships from the Children's Brittle Bone Foundation to X.Y., and from the Arthritis Foundation to X.Y., P.B., and T.S., respectively.

Received: September 5, 2003
Revised: March 1, 2004
Accepted: March 2, 2004
Published: April 29, 2004

References

Aubin, J.E., and Triffitt, J.T. (2002). Messenchymal Stem Cells and Osteoblat Differentiation, Vol. 1, 2nd ed. (San Diego: Academic Press).

Bonadio, J., Holbrook, K.A., Gelinas, R.E., Jacob, J., and Byers, P.H. (1985). Altered triple helical structure of type I procollagen in lethal perinatal osteogenesis imperfecta. J. Biol. Chem. *260*, 1734–1742.

Bruning, J.C., Gillette, J.A., Zhao, Y., Bjorbaeck, C., Kotzka, J., Knebel, B., Avci, H., Hanstein, B., Lingohr, P., Moller, D.E., et al. (2000). Ribosomal subunit kinase-2 is required for growth factor-stimulated transcription of the c-Fos gene. Proc. Natl. Acad. Sci. USA *97*, 2462–2467.

Coffin, R., Phillips, J.L., Staples, W.I., and Spector, S. (1966). Treatment of lead encephalopathy in children. J. Pediatr. *69*, 198–206.

Dalby, K.N., Morrice, N., Caudwell, F.B., Avruch, J., and Cohen, P. (1998). Identification of regulatory phosphorylation sites in mitogen-activated protein kinase (MAPK)-activated protein kinase-1a/p90rsk that are inducible by MAPK. J. Biol. Chem. *273*, 1496–1505.

De Cesare, D., Jacquot, S., Hanauer, A., and Sassone-Corsi, P. (1998). Rsk-2 activity is necessary for epidermal growth factor-induced phosphorylation of CREB protein and transcription of c-fos gene. Proc. Natl. Acad. Sci. USA *95*, 12202–12207.

Delepine, M., Nicolino, M., Barrett, T., Golamaully, M., Lathrop, G.M., and Julier, C. (2000). EIF2AK3, encoding translation initiation factor 2-alpha kinase 3, is mutated in patients with Wolcott-Rallison syndrome. Nat. Genet. *25*, 406–409.

Ducy, P., and Karsenty, G. (1995). Two distinct osteoblast-specific cis-acting elements control expression of a mouse osteocalcin gene. Mol. Cell. Biol. *15*, 1858–1869.

Ducy, P., Zhang, R., Geoffroy, V., Ridall, A.L., and Karsenty, G. (1997). Osf2/Cbfa1: a transcriptional activator of osteoblast differentiation. Cell *89*, 747–754.

Ducy, P., Starbuck, M., Priemel, M., Shen, J., Pinero, G., Geoffroy, V., Amling, M., and Karsenty, G. (1999). A Cbfa1-dependent genetic pathway controls bone formation beyond embryonic development. Genes Dev. *13*, 1025–1036.

Dufresne, S.D., Bjorbaek, C., El-Haschimi, K., Zhao, Y., Aschenbach, W.G., Moller, D.E., and Goodyear, L.J. (2001). Altered extracellular signal-regulated kinase signaling and glycogen metabolism in skeletal muscle from p90 ribosomal S6 kinase 2 knockout mice. Mol. Cell. Biol. *21*, 81–87.

Fisher, T.L., and Blenis, J. (1996). Evidence for two catalytically active kinase domains in pp90rsk. Mol. Cell. Biol. *16*, 1212–1219.

Frodin, M., Jensen, C.J., Merienne, K., and Gammeltoft, S. (2000). A phosphoserine-regulated docking site in the protein kinase RSK2 that recruits and activates PDK1. EMBO J. *19*, 2924–2934.

Gong, Y., Slee, R.B., Fukai, N., Rawadi, G., Roman-Roman, S., Reginato, A.M., Wang, H., Cundy, T., Glorieux, F.H., Lev, D., et al. (2001). LDL Receptor-Related Protein 5 (LRP5) Affects Bone Accrual and Eye Development. Cell *107*, 513–523.

Harding, H.P., Zhang, Y., Bertolotti, A., Zeng, H., and Ron, D. (2000). Perk is essential for translational regulation and cell survival during the unfolded protein response. Mol. Cell *5*, 897–904.

Harding, H.P., Zeng, H., Zhang, Y., Jungries, R., Chung, P., Plesken, H., Sabatini, D.D., and Ron, D. (2001). Diabetes mellitus and exocrine pancreatic dysfunction in perk-/- mice reveals a role for translational control in secretory cell survival. Mol. Cell *7*, 1153–1163.

Harding, H.P., Calfon, M., Urano, F., Novoa, I., and Ron, D. (2002). Transcriptional and translational control in the Mammalian unfolded protein response. Annu. Rev. Cell Dev. Biol. *18*, 575–599.

Harding, H.P., Zhang, Y., Zeng, H., Novoa, I., Lu, P.D., Calfon, M., Sadri, N., Yun, C., Popko, B., Paules, R., et al. (2003). An integrated stress response regulates amino acid metabolism and resistance to oxidative stress. Mol. Cell *11*, 619–633.

Hettmann, T., Barton, K., and Leiden, J.M. (2000). Microphthalmia due to p53-mediated apoptosis of anterior lens epithelial cells in mice lacking the CREB-2 transcription factor. Dev. Biol. *222*, 110–123.

Joel, P.B., Smith, J., Sturgill, T.W., Fisher, T.L., Blenis, J., and Lannigan, D.A. (1998). pp90rsk1 regulates estrogen receptor-mediated transcription through phosphorylation of Ser-167. Mol. Cell. Biol. *18*, 1978–1984.

Johnson, R.S., Spiegelman, B.M., and Papaioannou, V. (1992). Pleiotropic effects of a null mutation in the c-fos proto-oncogene. Cell *71*, 577–586.

Karsenty, G., and Wagner, E.F. (2002). Reaching a genetic and molecular understanding of skeletal development. Dev. Cell *2*, 389–406.

Kato, M., Patel, M.S., Levasseur, R., Lobov, I., Chang, B.H., Glass, D.A., 2nd, Hartmann, C., Li, L., Hwang, T.H., Brayton, C.F., et al. (2002). Cbfa1-independent decrease in osteoblast proliferation, osteopenia, and persistent embryonic eye vascularization in mice deficient in Lrp5, a Wnt coreceptor. J. Cell Biol. *157*, 303–314.

Kwok, C., Weller, P.A., Guioli, S., Foster, J.W., Mansour, S., Zuffardi, O., Punnett, H.H., Dominguez-Steglich, M.A., Brook, J.D., Young, I.D., et al. (1995). Mutations in SOX9, the gene responsible for Campomelic dysplasia and autosomal sex reversal. Am. J. Hum. Genet. *57*, 1028–1036.

Lee, B., Thirunavukkarasu, K., Zhou, L., Pastore, L., Baldini, A., Hecht, J., Geoffroy, V., Ducy, P., and Karsenty, G. (1997). Missense mutations abolishing DNA binding of the osteoblast-specific transcription factor OSF2/CBFA1 in cleidocranial dysplasia. Nat. Genet. *16*, 307–310.

Lowry, B., Miller, J.R., and Fraser, F.C. (1971). A new dominant gene mental retardation syndrome. Association with small stature, tapering fingers, characteristic facies, and possible hydrocephalus. Am. J. Dis. Child. *121*, 496–500.

Masuoka, H.C., and Townes, T.M. (2002). Targeted disruption of the activating transcription factor 4 gene results in severe fetal anemia in mice. Blood *99*, 736–745.

McKnight, S.L. (1992). CCAAT/Enhancer Binding Protein, Vol. 2. (New York: Cold Spring Harbor Laboratory Press).

McLeod, M.J. (1980). Differential staining of cartilage and bone in whole mouse fetuses by alcian blue and alizarin red S. Teratology *22*, 299–301.

Merienne, K., Jacquot, S., Zeniou, M., Pannetier, S., Sassone-Corsi, P., and Hanauer, A. (2000). Activation of RSK by UV-light: phosphorylation dynamics and involvement of the MAPK pathway. Oncogene *19*, 4221–4229.

Mundlos, S., Otto, F., Mundlos, C., Mulliken, J.B., Aylsworth, A.S., Albright, S., Lindhout, D., Cole, W.G., Henn, W., Knoll, J.H., et al. (1997). Mutations involving the transcription factor CBFA1 cause cleidocranial dysplasia. Cell *89*, 773–779.

Parfitt, A.M., Simon, L.S., Villanueva, A.R., and Krane, S.M. (1987). Procollagen type I carboxy-terminal extension peptide in serum as a marker of collagen biosynthesis in bone. Correlation with Iliac bone formation rates and comparison with total alkaline phosphatase. J. Bone Miner. Res. *2*, 427–436.

Poteet-Smith, C.E., Smith, J.A., Lannigan, D.A., Freed, T.A., and Sturgill, T.W. (1999). Generation of constitutively active p90 ribo-

somal S6 kinase in vivo. Implications for the mitogen-activated protein kinase-activated protein kinase family. J. Biol. Chem. *274*, 22135–22138.

Prockop, D.J., and Kivirikko, K.I. (1995). Collagens: molecular biology, diseases, and potentials for therapy. Annu. Rev. Biochem. *64*, 403–434.

Schinke, T., and Karsenty, G. (1999). Characterization of Osf1, an osteoblast-specific transcription factor binding to a critical cis-acting element in the mouse osteocalcin promoters. J. Biol. Chem. *274*, 30182–30189.

Sims, N.A., Dupont, S., Krust, A., Clement-Lacroix, P., Minet, D., Resche-Rigon, M., Gaillard-Kelly, M., and Baron, R. (2002). Deletion of estrogen receptors reveals a regulatory role for estrogen receptors-beta in bone remodeling in females but not in males. Bone *30*, 18–25.

Tanaka, T., Tsujimura, T., Takeda, K., Sugihara, A., Maekawa, A., Terada, N., Yoshida, N., and Akira, S. (1998). Targeted disruption of ATF4 discloses its essential role in the formation of eye lens fibres. Genes Cells *3*, 801–810.

Temtamy, S.A., Miller, J.D., and Hussels-Maumenee, I. (1975). The Coffin-Lowry syndrome: an inherited faciodigital mental retardation syndrome. J. Pediatr. *86*, 724–731.

Trivier, E., De Cesare, D., Jacquot, S., Pannetier, S., Zackai, E., Young, I., Mandel, J.L., Sassone-Corsi, P., and Hanauer, A. (1996). Mutations in the kinase Rsk-2 associated with Coffin-Lowry syndrome. Nature *384*, 567–570.

Wang, Z.Q., Ovitt, C., Grigoriadis, A.E., Mohle-Steinlein, U., Ruther, U., and Wagner, E.F. (1992). Bone and hematopoietic defects in mice lacking c-fos. Nature *360*, 741–745.

Xing, J., Ginty, D.D., and Greenberg, M.E. (1996). Coupling of the RAS-MAPK pathway to gene activation by RSK2, a growth factor-regulated CREB kinase. Science *273*, 959–963.

Young, I.D. (1988). The Coffin-Lowry syndrome. J. Med. Genet. *25*, 344–348.

Zhang, P., McGrath, B., Li, S., Frank, A., Zambito, F., Reinert, J., Gannon, M., Ma, K., McNaughton, K., and Cavener, D.R. (2002). The PERK eukaryotic initiation factor 2 alpha kinase is required for the development of the skeletal system, postnatal growth, and the function and viability of the pancreas. Mol. Cell. Biol. *22*, 3864–3874.